

Article

Preliminary Design and Analysis of a Photovoltaic-Powered Direct Air Capture System for a Residential Building

Anwar Hamdan Al Assaf ¹, Odi Fawwaz Alrebei ², Laurent M. Le Page ³, Luai El-Sabek ⁴, Bushra Obeidat ⁵, Katerina Kaouri ⁶, Hamed Abufares ² and Abdulkarem I. Amhamed ^{2,*}

¹ Department of Aviation Sciences, Amman Arab University, Amman 11953, Jordan

² Qatar Environment and Energy Research Institute (QEERI), Hamad Bin Khalifa University, Doha 34110, Qatar

³ Oxford Thermofluids Institute, Oxford University, Oxford OX2 OES, UK

⁴ Lean Construction Institute—Qatar, Doha 23850, Qatar

⁵ College of Architecture and Design, Jordan University of Science and Technology, Irbid 22110, Jordan

⁶ School of Mathematics, Cardiff University, Cardiff CF24 4AG, UK

* Correspondence: aamhamed@hbku.edu.qa

Abstract: To promote the adoption of Direct Air Capture (DAC) systems, this paper proposes and tests a photovoltaic-powered DAC system in a generic residential building located in Qatar. The proposed DAC system can efficiently reduce CO₂ concentration in a living space, thus providing an incentive to individuals to adopt it. The ventilation performance of the building is determined using Computational Fluid Dynamics (CFD) simulations, undertaken with ANSYS-CFD. The CFD model was validated using microclimate-air quality dataloggers. The simulated velocity was 1.4 m/s and the measured velocity was 1.35 m/s, which corresponds to a 3.5% error. The system decarbonizes air supplied to the building by natural ventilation or ventilation according to the ASHRAE standards. Furthermore, the performance of the photovoltaic system is analyzed using the ENERGYPLUS package of the Design Builder software. We assume that 75% of CO₂ is captured. In addition, a preliminary characterization of the overall system's performance is determined. It is determined that the amount of CO₂ captured by the system is 0.112 tones/year per square meter of solar panel area. A solar panel area of 19 m² is required to decarbonize the building with natural ventilation, and 27 m² is required in the case of ventilation according to the ASHRAE standard.

Keywords: direct air capture systems; carbon capture and storage; energy analysis; computational fluid dynamics analysis; living space



Citation: Al Assaf, A.H.; Alrebei, O.F.; Le Page, L.M.; El-Sabek, L.; Obeidat, B.; Kaouri, K.; Abufares, H.; Amhamed, A.I. Preliminary Design and Analysis of a Photovoltaic-Powered Direct Air Capture System for a Residential Building. *Energies* **2023**, *16*, 5583. <https://doi.org/10.3390/en16145583>

Academic Editor: Pål Østebo Andersen

Received: 13 June 2023

Revised: 18 June 2023

Accepted: 21 June 2023

Published: 24 July 2023



Copyright: © 2023 by the authors. Licensee MDPI, Basel, Switzerland. This article is an open access article distributed under the terms and conditions of the Creative Commons Attribution (CC BY) license (<https://creativecommons.org/licenses/by/4.0/>).

1. Introduction

Recent research has clearly demonstrated that a swift and comprehensive transition to renewable energy systems is essential for achieving a 1.5–2 °C reduction in temperature [1], as per the desired global energy transition [1]. The Paris Agreement, adopted by the United Nations Framework Convention on Climate Change (UNFCCC) in 2015, aims to strengthen the ability of countries to deal with the impacts of climate change and to accelerate and intensify the actions and investment needed for a sustainable low carbon future. However, atmospheric carbon prevents us from meeting these goals. In [1], it is estimated that the direct air capture of CO₂, commonly known as negative emission (NE)), requirement will be around 10,000 megatons of CO₂ in the next 25 years, followed by 10,000 additional megatons by the end of this century. This suggests that the capacity for non-emitting energy sources (NEES) should be increased within the next 15 years; substantial investments will be necessary to achieve this by 2050. As recently observed in [2], and fully endorsed by the Intergovernmental Panel on Climate Change (IPCC) [3,4], most of the integrated assessment models (IAMs) heavily depend on bio-energy carbon capture and storage (BECCS) systems; they generally do not consider CO₂ reduction through Direct Air Capture (DAC).

However, various obstacles hinder the extensive implementation of BECCS. These obstacles include the need for substantial land areas due to the BECCS' low area efficiency, high water usage, a strain on the energy system caused by low energy return on investment, and the high cost of bioenergy-based sources [5–8].

In addition, BECCS as an inflexible base power-generation technology would not add much to an energy system that is primarily based on inexpensive, sustainable energy sources, such as solar and wind energy, which require flexibility [6,9,10]. According to [11,12], future power systems will rely, to a very large extent, on variable renewable energy (VRE) and may be less expensive than most current energy systems. In 2018, for the first time, it was concluded by the IPCC that systems entirely based on renewable energy (RE) must be seriously considered.

The technological practicality and profitability of 100% RE systems, particularly for the electricity industry, were highlighted in [11]; most research in highly renewable shares supports the need for sustainable bio-energy alternatives [11–13].

Electricity-powered DAC alternatives have not received significant attention in IAMs. This may be explained by the underappreciated contribution of VRE to mitigating climate change [14]. However, current growth in the adoption of VRE [15] may prompt more attention to DAC and IAMs in the short term and lead to satisfactory solutions. DAC systems can combine several desired characteristics, including a large area footprint for large-scale deployment, minimal conflicts with land use, and a great fit with future electricity-based RE systems, based on solar (PV) or wind energy [15–19]. This suggests further significant benefits, including a very cheap energy supply, strong energy system integration, accessibility to regions with abundant energy resources, and the ability to decouple the sites of DAC and power production, if necessary. In contrast to conventional CO₂ capture methods, such as amine-based post-combustion capture, DAC is gaining popularity, since it has enormous potential and great flexibility to collect CO₂ from discrete sources as a “synthetic tree”. It is one of the newer carbon capture technologies that has emerged in recent years, although it is still in the prototype study stage and faces several technical obstacles. The state-of-the-art of DAC and CO₂ management was thoroughly discussed by L. Jiang et al. [18], who also noted technological limitations and provided inquiry prospects for large-scale commercial applications. In addition, evaporation/condensation heat of the vapor compression refrigeration (VCR) cycle in the air conditioning system of buildings was recommended by Ying Ji et al. [19] for the adsorption/desorption process of DAC in order to further increase thermal performance. Ying Ji et al. examined the thermal performance of a four-step temperature swing adsorption method (TSA) at varied adsorption/desorption temperatures utilizing various adsorbents. In an effort to find a balance between the adsorbent and the refrigerant, they also performed an analysis of the Coefficient of Performance (COP) of the VCR cycle.

Although a RE-powered DAC system has been proposed in the literature, incentives at the individual level or to the carbon-emitting industries that have to abide to national/international regulations for reducing CO₂ emissions, are not clear. The industries mainly use conventional Carbon Capture and Storage (CCS) technologies, which prevent increases, but do not reduce the existing CO₂ footprint in the same way as DAC systems. Therefore, to promote the adoption of DAC systems, here, we propose a system composed of a generic residential building (located in Qatar) equipped with a photovoltaic-powered DAC system that efficiently achieves a reduction of the CO₂ content in a specific living space. This should provide direct motivation for individuals to adopt a DAC system. The ventilation performance of the building has been determined through Computational Fluid Dynamics analysis using ANSYS-CFD. The performance of the photovoltaic system has been analyzed using the ENERGYPLUS package of the DesignBuilder software [20].

2. Materials and Methods

2.1. System Description (DAC)

The proposed system comprises three subsystems: a DAC system, a photovoltaic system, and a generic building, as shown in Figure 1. The DAC system has been proposed

in [19]. It directly captures CO_2 from the atmospheric air and supplies a building with decarbonized air. We assume that 75% of the CO_2 content is captured [19]. The DAC system is powered by the photovoltaic system and comprises four main units: an air contactor, a pellet reactor, a calciner, and a slaker. The air contactor captures CO_2 by forcing air to contact an alkali liquid. Once the air contacts the alkali liquid, a diffusion reaction occurs that leads to the capture of CO_2 . The mass transfer coefficient (K_L) has been estimated in [19] to be approximately 0.13 cm/s at 293 K.

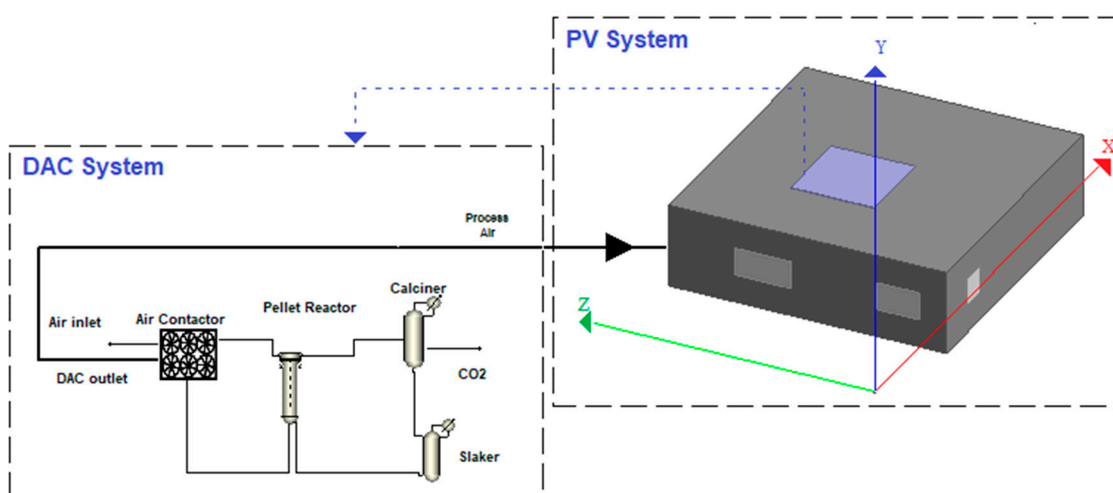


Figure 1. Schematic of the DAC system powered by the photovoltaic system.

The mixture content in the air contactor is 1 M OH^- , 0.5 M CO_3^{2-} , and 2 M K^+ . The resultant reaction that occurs in the air contactor reacts every CO_2 mol with two mol of KOH to produce one mol of H_2O and one mol of K_2CO_3 . The resultant K_2CO_3 from the contactor reaction is transferred to the pellet reactor, in which each mol of K_2CO_3 is reacted with one mol of $\text{Ca}(\text{OH})_2$ in an exothermic reaction (-5.8 kJ/mol) to produce two mol of KOH and one mole of CaCO_3 . The former is recycled back to the air contactor, and the latter is fed into the calciner to be transformed into CO_2 and CaO in an endothermic process ($+178.3$ kJ/mol). The latter is supplied to the slaker to react each mole of CaO with one mole of H_2O in the exothermic process to produce $\text{Ca}(\text{OH})_2$. The latter is recycled back to the pellet reactor. According to [19], the DAC system consumes approximately 8.81 GJ of natural gas to capture one ton of CO_2 ; this corresponds to approximately 2.45 MWh. For capturing one ton of CO_2 , the rate of air capture should be approximately 2.194×10^6 kg/h. The photovoltaic system is modeled in DesignBuilder [20], assuming constant efficiency for the PV (option “PV constant efficiency”). The methodology is detailed in Section 2.2.

2.2. System Description (Photovoltaic System)

DesignBuilder was utilized in this study to assess the photovoltaic system’s efficiency. DesignBuilder (EnergyPlus package) is the favored software for analyzing a building’s energy performance amongst architects, engineers, and other professionals; it is considered the industry standard for Building Energy Simulation [21]. The software enables users to perform comprehensive energy simulations using a 3D interface. DesignBuilder’s energy modeling accuracy has been certified by BESTest of the International Energy Agency [22]. The U.S. Department of Energy and the global community use BESTest to assess software for building energy modeling [23]. The simulation incorporates diverse sub-hourly regional climatic and environmental factors [21–24]. The photovoltaic model is built with the “PV constant efficiency” option, as mentioned in Section 2.1. The parameter values used in the generic residential building and photovoltaic system models are summarized in Table 1 and Table 2, respectively.

The performance of the PV system was evaluated for a generic residential building in Doha, Qatar. The weather data, displayed in Figure 2, was loaded into DesignBuilder, following [25]. Information regarding the accuracy of this weather data can be found in open-access sources [25]. The data are post-processed from the TMYx files available in [25]. TMYx is typical hourly weather data from 2021 in the ISD (U.S. NOAA's Integrated Surface Database), obtained using the TMY/ISO 15927-4:2005 methodologies [25].

As suggested in [26,27], to generate accurate results, DesignBuilder has been configured to execute an annual solar energy simulation with 30 steps per hour.

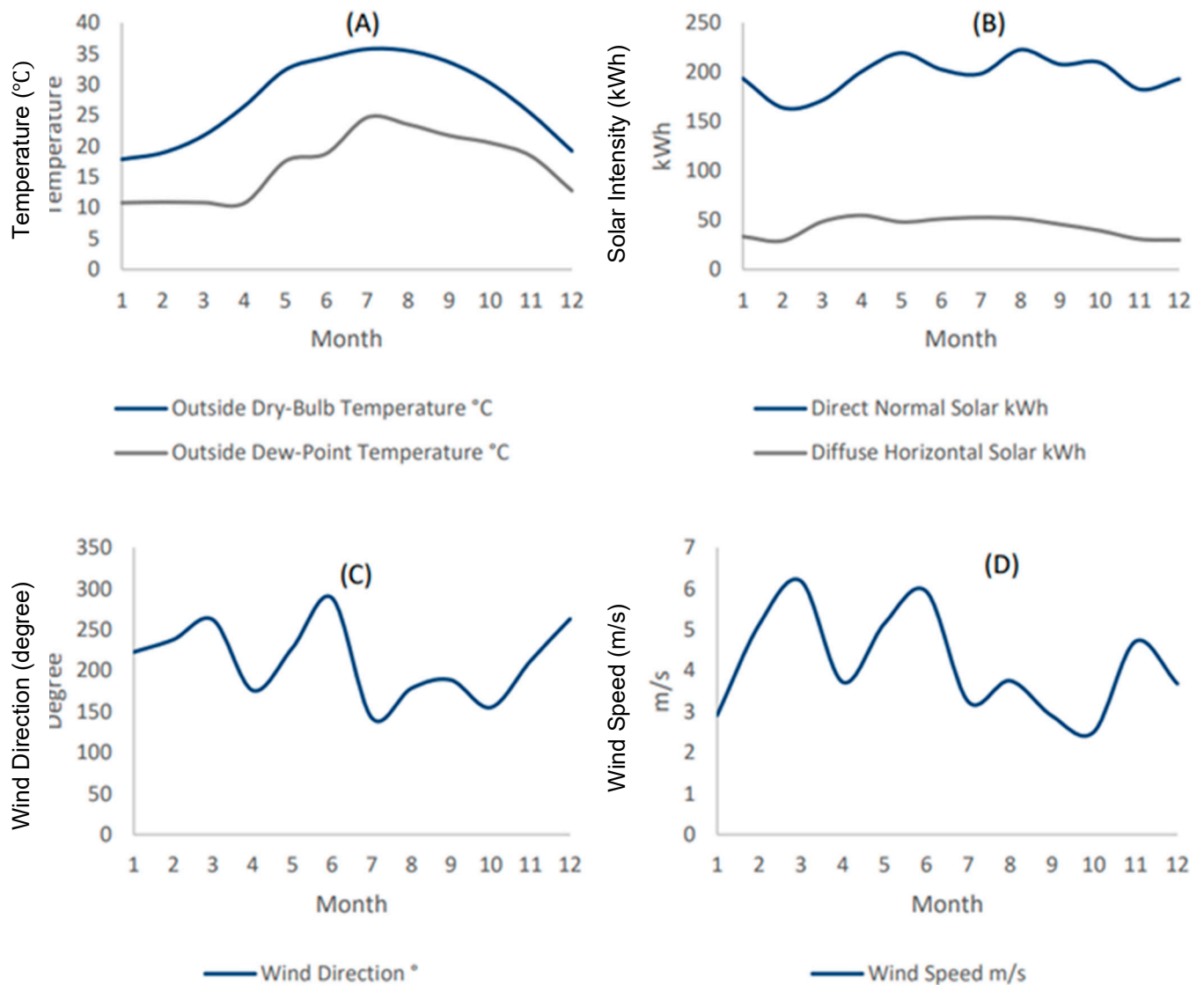


Figure 2. Cont.

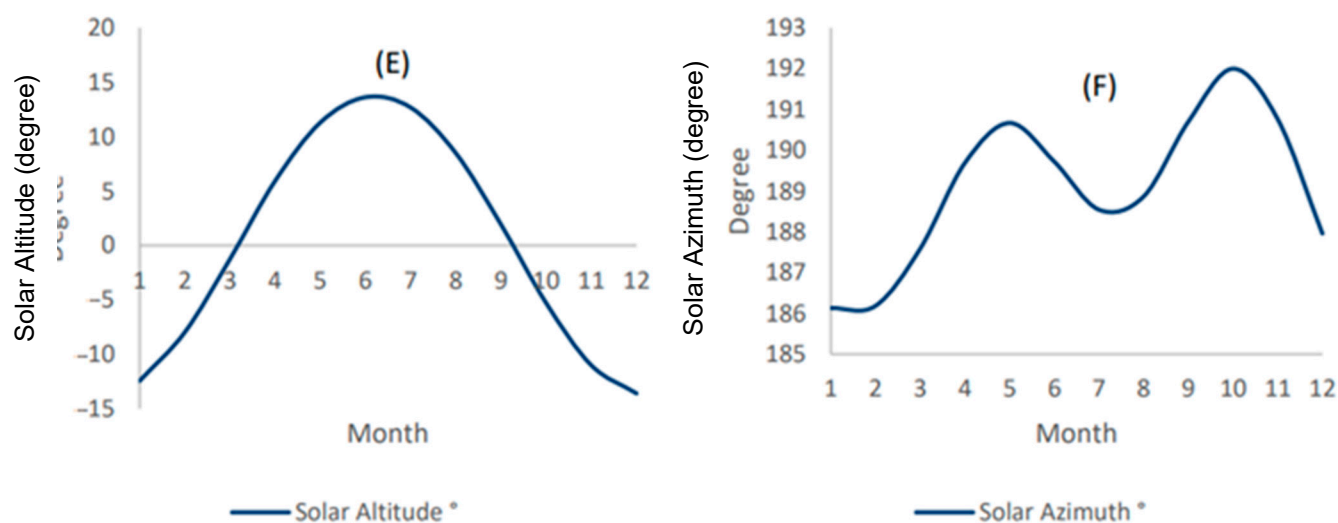


Figure 2. Site weather data (Doha, Qatar). (A) Outside dry-bulb and dew-point temperatures. (B) Direct normal and diffusive horizontal solar intensity. (C) Wind direction. (D) Wind speed. (E) Solar altitude. (F) Solar Azimuth.

2.3. System Description (Generic Residential Building)

The building under consideration (see Figure 3A) is a generic residential building in Qatar that has been described in detail in previous work [26,27].

The proposed DAC system is designed to capture all of the CO₂ from the air that is supplied to the building through ventilation. Therefore, to determine the required capacity of the DAC system and the corresponding energy required, the natural ventilation rate, V_{act} , is quantified below. The ventilation settings are assumed to be as in [26,27]; see Section 3.1.

Previous CFD studies [26,27] have used ANSYS-CFX to calculate the ventilation rate of the building considered here. The weather conditions—average temperature and total wind velocity—were taken from [28]; these were 27.8 °C and 4.2 m/s, respectively. The total wind velocity on the building was modeled as in [26,27,29,30], with equal shear and normal velocities (i.e., $V_x = V_z = 2.97$ m/s); see Figure 4. The Boolean technique was applied by subtracting the solid domain from the fluid domain in [27,28]. The CAD model is generated utilizing AutoCAD.

Mesh-sensitivity analysis is performed to verify the accuracy of the simulations, utilizing the average air velocity. The results have been shown to be independent of the resultant mesh size. The number of elements was determined based on mesh sensitivity analysis—mesh independence was achieved at approximately 9.4×10^5 elements—see also Figure 3. [26,27]. However, a finer mesh with 2.19×10^6 elements was selected for the simulation to ensure a high level of confidence and accuracy. More information about the CFD setup of the generic building model can be found in [26,27,29,30]. Table 1 shows the CFD simulation assumptions and setups. Furthermore, it is shown in Figure 3 that reducing the mesh size results in a decrease in the relative error, as required (i.e., the air velocity values achieved convergence with a relative error margin of 1%).

Table 1. CFD simulation assumptions, setup, and parameter values.

Category	Property	Specification
Mesh Quality	Elements maximum size (mm)	500
	Number of elements	2,190,000
	Growth rate	1.2
	Defeature size (mm)	2.5
	Curvature minimum size (mm)	5

Table 1. Cont.

Category	Property	Specification
	Curvature normal angle (degree)	18
	Skewness	0.21188
	Orthogonal quality	0.78694
	Inflation transition ratio	0.75
	Inflation number of layers	5
Turbulence model	$k - \epsilon$	$k = \frac{3}{2}(UI)^2$ $\epsilon = c_{\mu}^{\frac{3}{4}}k^{\frac{3}{2}}l^{-1}$ $l = 0.16Re^{-\frac{1}{8}}$ $l = 0.07L$
Solid Modeling	Domain Solid-fluid Inlet conditions	Boolean No-Slip Walls Velocity inlets; as per Figure 5, with a turbulence intensity of 5%
Fluid Modeling and Boundary Conditions	Outlet condition External surfaces of the computational domain	Pressure outlets of 1 bar Openings An open boundary condition is a computational boundary that allows phenomena generated in the interior domain to pass through the artificial boundary without distortion and without affecting the interior solution.
Computational performance	Computational performance Computational time Software Residual targets Achieved residual level	Computational performance 12 h/case Ansys CFX 1×10^{-3} Approximately 1×10^{-6}
Boundary Wall Simulation	No slip wall Steady state	Smooth
CFD assumptions	As detailed in [26,27,29,30]	[26,27,29,30].

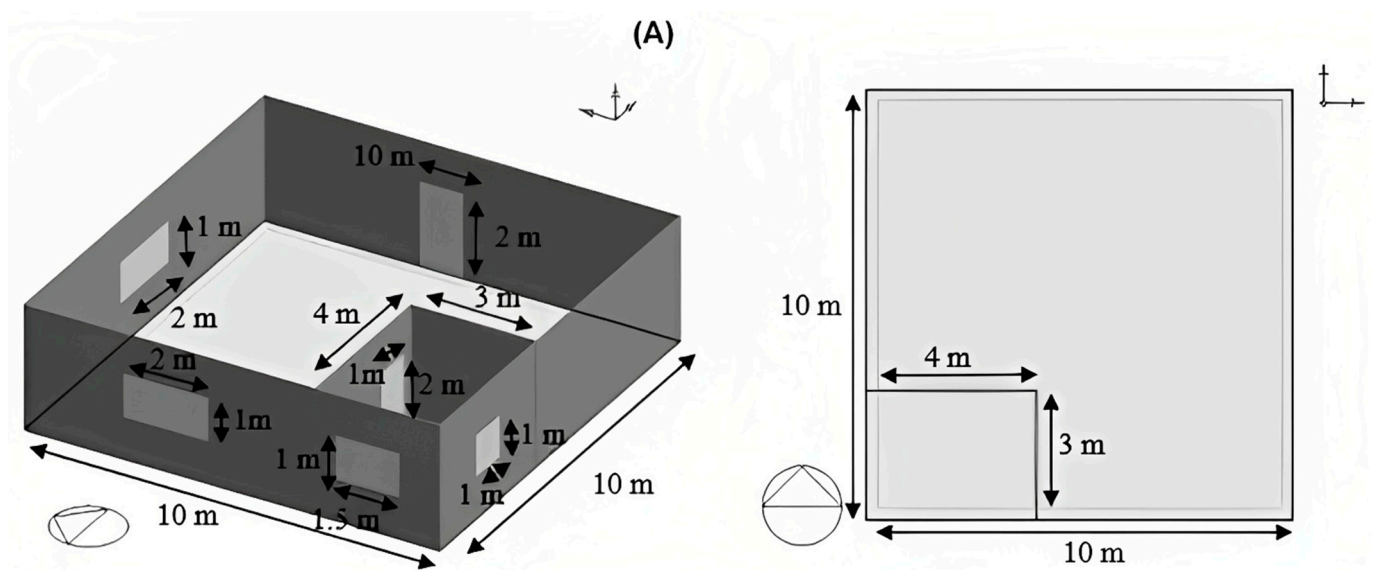


Figure 3. Cont.

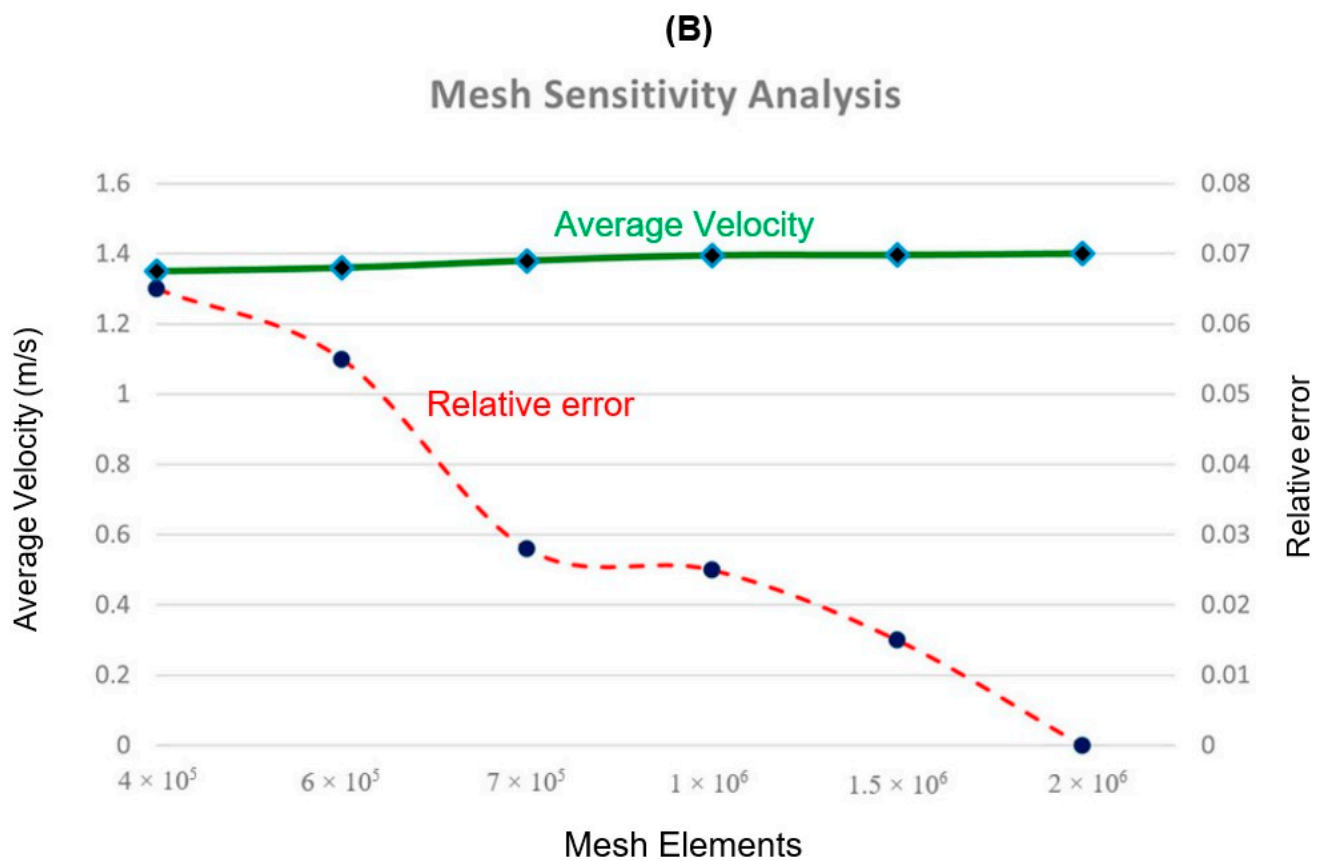


Figure 3. (A) The 3D model and top-down plan for the generic building considered, as built in DesignBuilder. (B) Mesh sensitivity analysis.

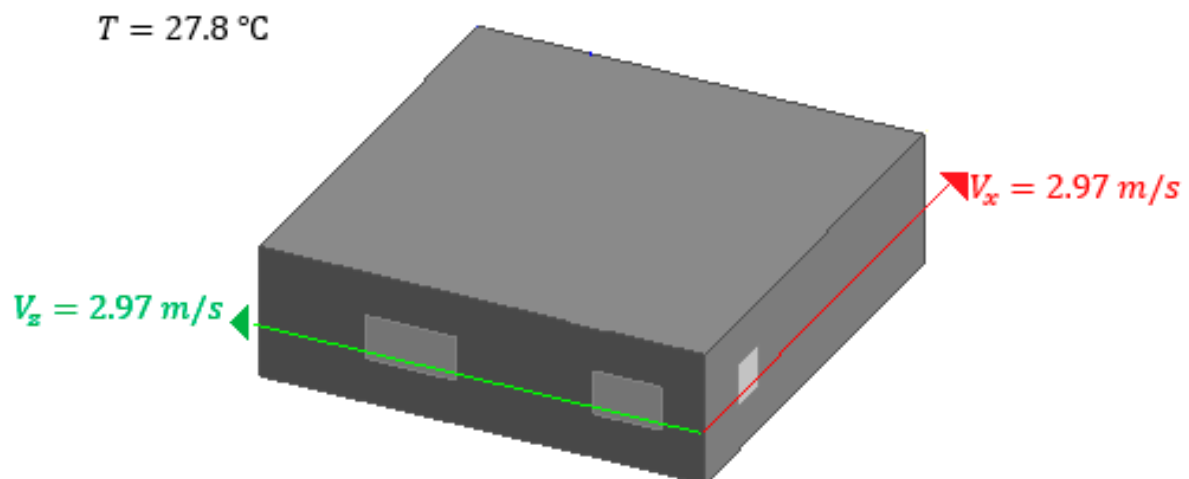


Figure 4. The geometry of the building, as used in the CFD model. The air comes into the building through natural ventilation. The normal and shear air velocities on the building are shown. The temperature is assumed to be $27.8 \text{ }^\circ\text{C}$.

The DeltaOhm datalogger for microclimate—air quality analysis [31] was used to validate the CFD model. The instrument measures air velocity using an Omnidirectional hotwire probe. The velocity range has been determined to be 0.02–5 m/s, used for PMV measurement [32]. The setup is shown in Figure 5. The measured velocity was 1.35 m/s and the simulated velocity was 1.4 m/s which corresponds to an estimated error of 3.5%.



Figure 5. DeltaOhm datalogger fitted with Omnidirectional hotwire probe.

2.4. Numerical Model Specifications and Assumptions

Here, we summarize all of the assumptions we adopted for the three subsystems, described in Section 2.1–2.3; i.e., the DAC system, the Photovoltaic system, and the generic residential building. Details justifying these assumptions are found in the references provided in Table 2.

Table 2. Assumptions adopted for the three subsystems (DAC system, Photovoltaic system, and generic building).

Parameter	DAC System	
	Value	Reference
Subunits	Air contractor, Pellet reactor, Calciner, and Slaker	[19]
Mass transfer coefficient (KL)	0.13 cm/s (293 K)	[19]
Mixture content in the air contractor	1 M OH ⁻ , 0.5 M CO ₃ ²⁻ , and 2 MK ⁺	[19]
Reaction in the air contractor	CO ₂ + KOH → H ₂ O + K ₂ CO ₃	[19]
Reaction in the pellet reactor	K ₂ CO ₃ + Ca(OH) ₂ → 2KOH + CaCO ₃	[19]
Reaction in the calciner	CaCO ₃ → CO ₂ and CaO	[19]
Reaction in the slaker	CaO + H ₂ O → Ca(OH) ₂	[19]
Energy consumption to capture 1 ton of CO ₂	2.45 MWh	[19]
Air flowrate needed to capture 1 ton of CO ₂	2.194 × 10 ⁶ kg/h	[19]
Percentage of captured CO ₂	75%	[19]
DAC-Building integration	CO ₂ captured from ducts transferring air to and from the rooms	Proposed

Table 2. Cont.

DAC System			
Parameter	Value	Reference	
Photovoltaic system			
Parameter	Value	Reference	
PV efficiency (η_{pv})	15%	[20]	
Inverter efficiency (η_I)	95%	[20]	
Fraction of surface with active solar cells (A_{act}/A_{PV})	90%	[20]	
Total solar panel area (A_{PV})	1–27 m ²	[20]	
Depth (D)	0.025 m	[20]	
Tilting	Fixed horizontal	[20]	
Mounting system for installing photovoltaic	Roof-Solar Bitumen	[20]	
Operation scheme	Base load (operates even if the electric power generated is greater than the building demand)	[20]	
Electric Bus type	Direct Current with inverter	[20]	
Conditions of the generic building			
Average outside temperature	27.8 °C	[26]	
Total wind velocity	4.2 m/s	[27]	
Shear and normal velocity, V_x, V_z	2.97 m/s	[28]	

3. Results

3.1. Ventilation Performance

As discussed in Section 2.3, the natural ventilation rate obtained through our CFD analysis (see Figure 6) was used to determine the required capacity of the DAC system and the corresponding energy required to decarbonize the air supplied to the building. The air velocity contours and streamlines were plotted at two planes inside the building (1 m and 1.7 m above ground), as in [26,27]. Subsequently, the average velocity and the total ventilation rate were estimated and are displayed in Figure 7.

The average air velocity at the 1-m and 1.7-m planes is found to be approximately 1.33 m/s and 1.06 m/s, respectively. The ventilation rate, V_{act} , is estimated to be 532.97 kg/h, which is equivalent to 4669 tons of air per year. This implies that the photovoltaic-powered DAC can effectively decrease carbon emissions. According to [19], the DAC system consumes approximately 8.81 GJ of natural gas to capture one ton of CO₂, which corresponds to $P_{DAC} = 2.45$ MW of electric power. The air to capture this content of CO₂ is approximately $V_{DAC} = 2194$ tons at STP “Standard Temperature and Pressure”. Therefore, the power to airflow ratio that fully decarbonizes the air entering the building is $P_{DAC}/V_{DAC} = 0.001$ MW/n. Hence, the power required to decarbonize the air that would have been supplied to the building through natural ventilation over a year is $P_{act} = V_{act} \times \frac{P_{DAC}}{V_{DAC}} = 5.21$ MW.

3.2. Photovoltaic System Performance

As discussed in Section 3.1, to decarbonize the air supplied to the building by 75% through natural ventilation, the DAC system’s power should be $P_{act} = 5.21$ MW/year. Therefore, the performance of the photovoltaic system is estimated herein for a 1 m² solar panel; see Figure 8.

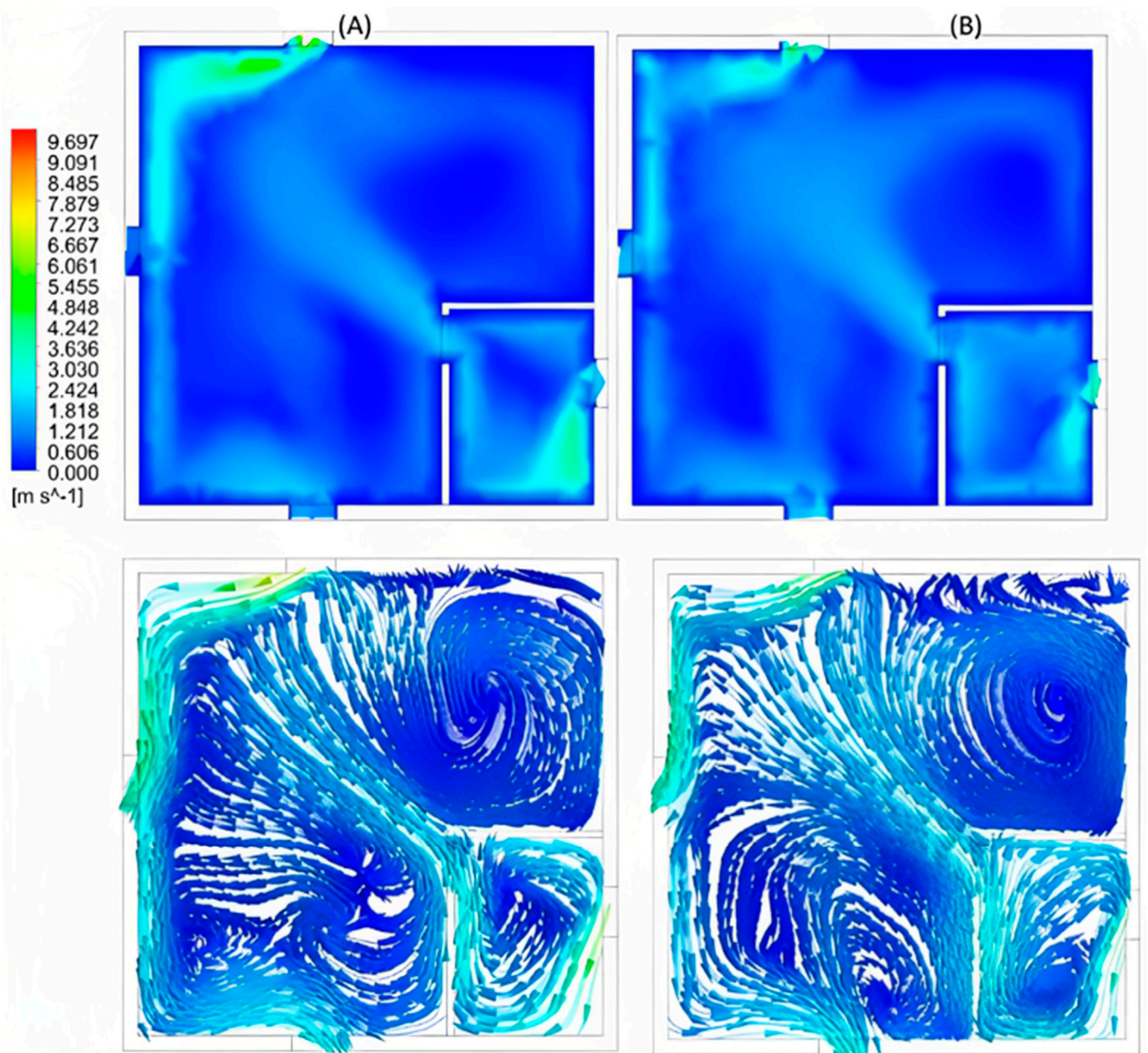


Figure 6. Air velocity contours and streamlines inside the building, at (A) 1 m and (B) 1.7 m above ground, generated through CFD analysis in ANSYS-CFX.

We find that the total annual power generated by a 1-m² solar panel photovoltaic system is approximately $\bar{P}_v = 0.2746$ MW/year·m² (see Figure 8).

It is assumed that the designed photovoltaic system's power output is linearly related to the size of the solar panel area (A_{PV}). Therefore, the required solar panel area that can allow full decarbonization of the air supplied to the building is approximately $\frac{P_{act}}{\bar{P}_v} = 19$ m². This is determined by plotting the power production for the solar panel area taken to be 1–27 m², with a step size of 1 m²; see Figure 9. Figure 10 shows a linear relationship; the power sensitivity of the photovoltaic system with respect to the solar-panel area ($\partial P_{act} / \partial A_{PV}$) is approximately 0.275 MW/year·m², which is equivalent to the total annual power generated by a 1-m² solar panel photovoltaic system, \bar{P}_v .

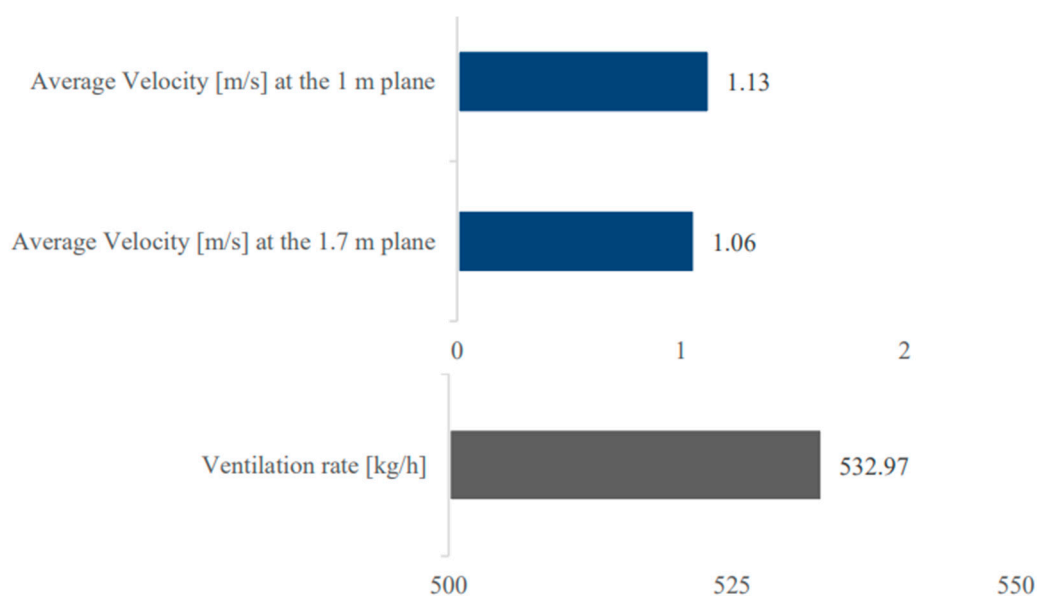


Figure 7. Actual ventilation rate and the average velocity at 1 m and 1.7 m.

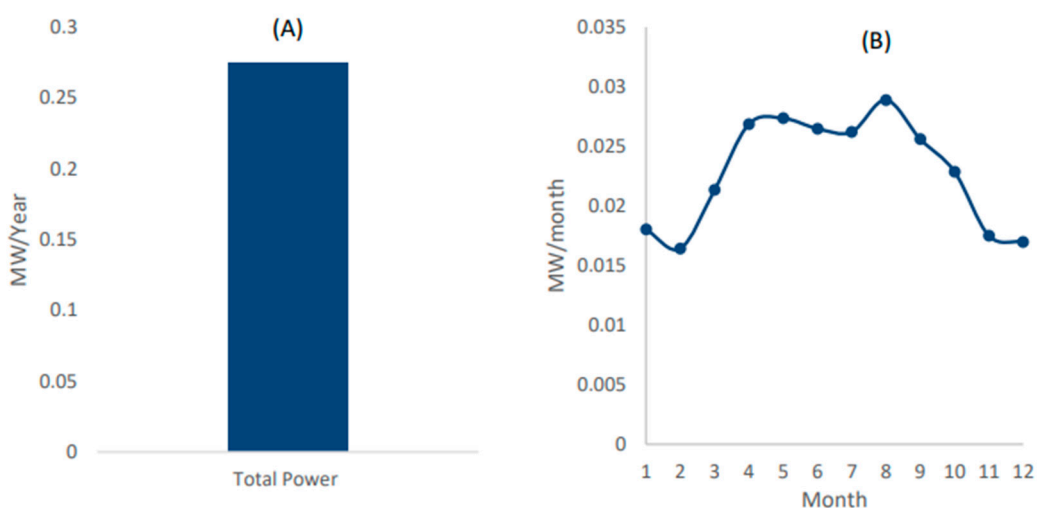


Figure 8. (A) The total annual power generated by a 1-m² solar panel photovoltaic system (\bar{P}_v). (B) The monthly power breakdown generated by a 1-m² solar panel photovoltaic system.

In addition, as shown in Figure 10, with a solar panel area of 19 m², the photovoltaic system generates the required annual power to run the DAC system to decarbonize air supplied to the building through natural ventilation (i.e., 5.21 MW/year to decarbonize 4669 ton/year).

According to [19], the DAC system consumes approximately 2.45 MW to capture one ton of CO₂. As shown in Figure 10, the solar panel area of the photovoltaic system required to generate the required annual power to capture one ton of CO₂ is approximately 9 m².

Another crucial design criterion is to estimate the required power and solar panel area to decarbonize the required ventilation rate of the building. The ventilation rate required in the building is recommended by the American Society of Heating, Refrigerating, and Air-Conditioning Engineers (ASHRAE) standards. According to [26,27], the required ventilation rate of the adopted generic building based on the ASHRAE standards is approximately $V_{ASHRAE} = 6642$ tons/year of air. The corresponding CO₂ content is 3.03 tons/year. According to [19], the power to the captured CO₂ ratio is 2.45 MW/ton; thus, the required power to decarbonize V_{ASHRAE} is approximately 7.41 MW/year. As shown in Figure 10,

the photovoltaic system with a solar panel area of 27 m² has the capability of generating 7.41 MW/year.

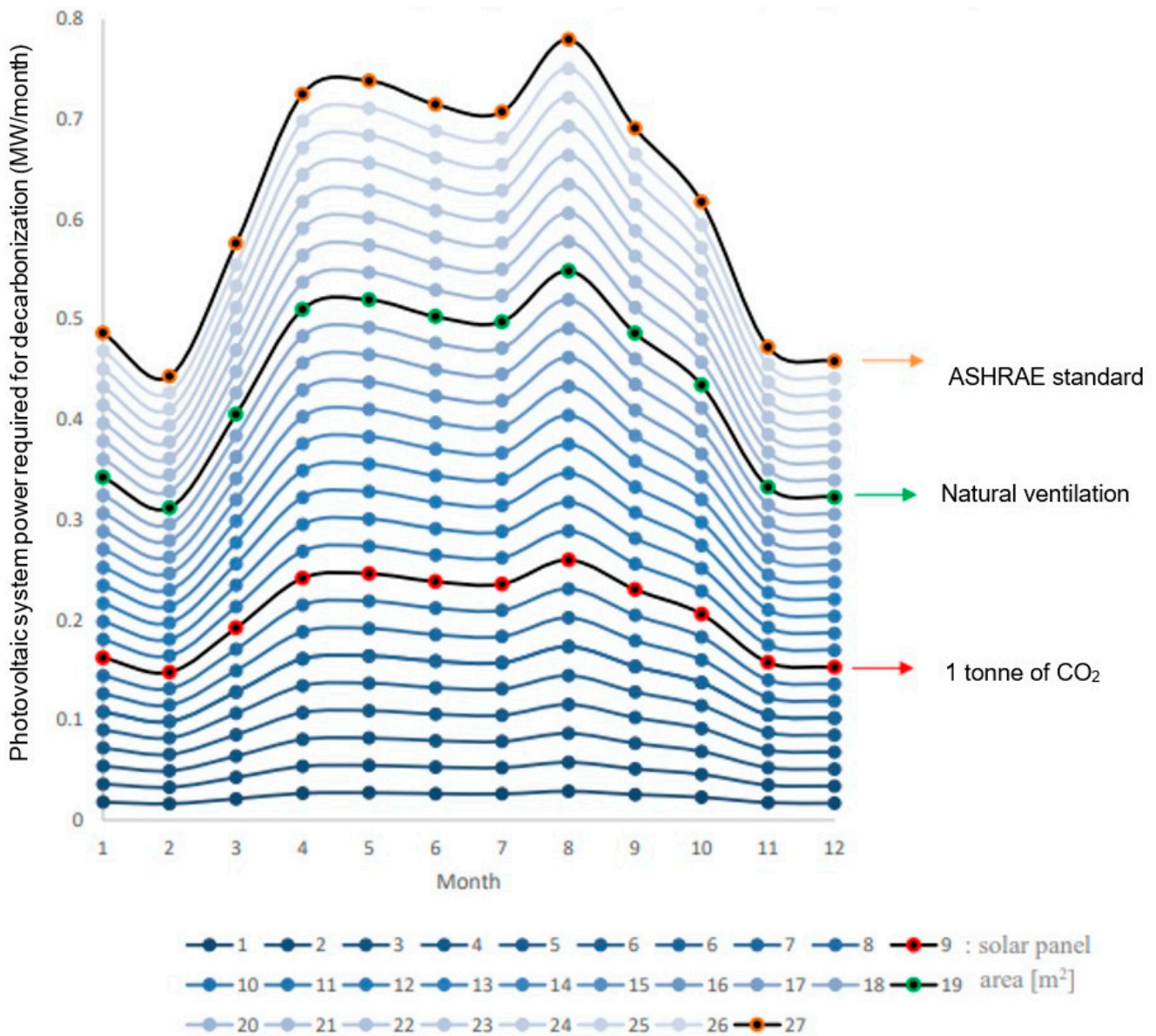


Figure 9. The monthly breakdown of the power generated by a photovoltaic system with solar-panel areas of 1–27 m².

Since the ratio of the power required to the captured CO₂ is 2.45 MW/ton [19], the annual captured CO₂ amount (m_{CO_2}) by the available power of each photovoltaic has been estimated in Figures 10 and 11. As shown in Figure 11, the sensitivity of the captured amount of CO₂ with respect to the solar panel area is $\partial m_{CO_2} / \partial A_{PV} = 0.112$ tons/year.m². This means that increasing the solar panel area of the photovoltaic system by 1 m² enables the DAC system to capture an additional 0.112 tons/year of CO₂.

National and international regulations dictate the capture of CO₂ emissions generated by industrial plants. Driven by these regulations and national and international law, the industry has adopted carbon capturing and storage (CCS) methods. However, the usual CCS techniques are the conventional post-combustion [33–35], pre-combustion [36–38], and oxyfuel combustion [39,40] methods, which are preventive, but not corrective methods; that is, they cannot lead to zero carbon emissions and, thus, cannot reduce the existing

global carbon footprint. In contrast, implementing the DAC system is a corrective action (i.e., a negative-carbon-emission system) as it directly removes CO₂ from the atmosphere, reducing the global carbon footprint.

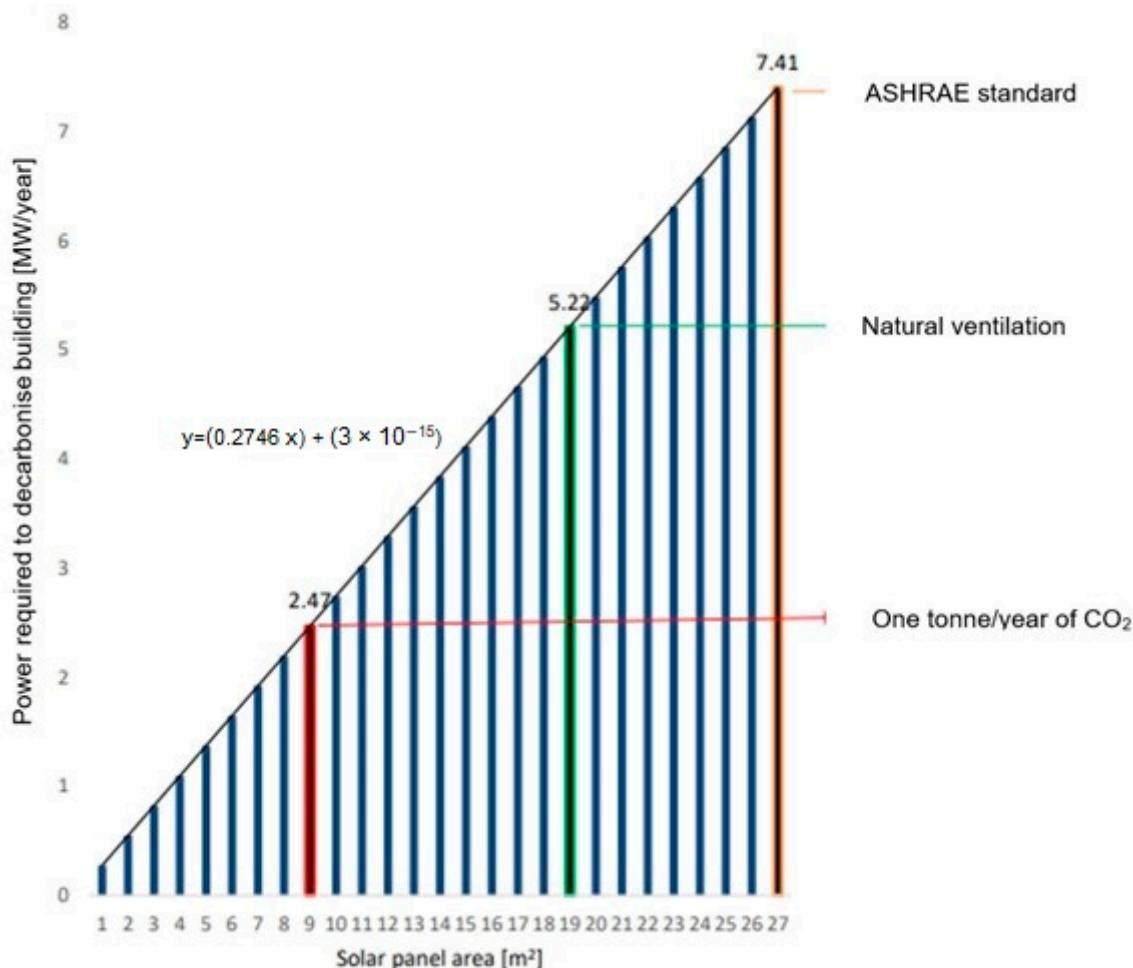


Figure 10. The total annual power generated by a photovoltaic system with a solar panel area of 1–27 m².

However, without binding international regulations, the main obstacle that faces the implementation of DAC systems on a wide scale is identifying motivating factors for individuals to adopt them. While the concept of a renewable-energy-powered DAC system has been proposed in the literature, clear incentives for individuals were not previously given. We propose a photovoltaic-powered DAC system that efficiently reduces the CO₂ content in a living space, thus, providing the incentive for adoption at the individual level. The proposed system is also attractive at the national/international level.

Here, the power of the photovoltaic system to enable the DAC system to decarbonize the ventilation flow was determined for a residential building. To decarbonize the natural ventilation airflow (V_{act}), the solar panel area was found to be 19 m² and the corresponding power to be 5.22 MW/year; the DAC system then captures 2.13 tons/year of CO₂. In addition, to decarbonize the airflow corresponding to the ASHRAE standard (V_{ASHRAE}), the solar panel area was found to be 27 m² and the corresponding power to be 7.4 MW/year; the DAC system then captures 3.03 tons/year of CO₂. Moreover, the 9-m² solar panel area generates 2.47 MW/year, enabling the DAC to capture one ton/year of CO₂.

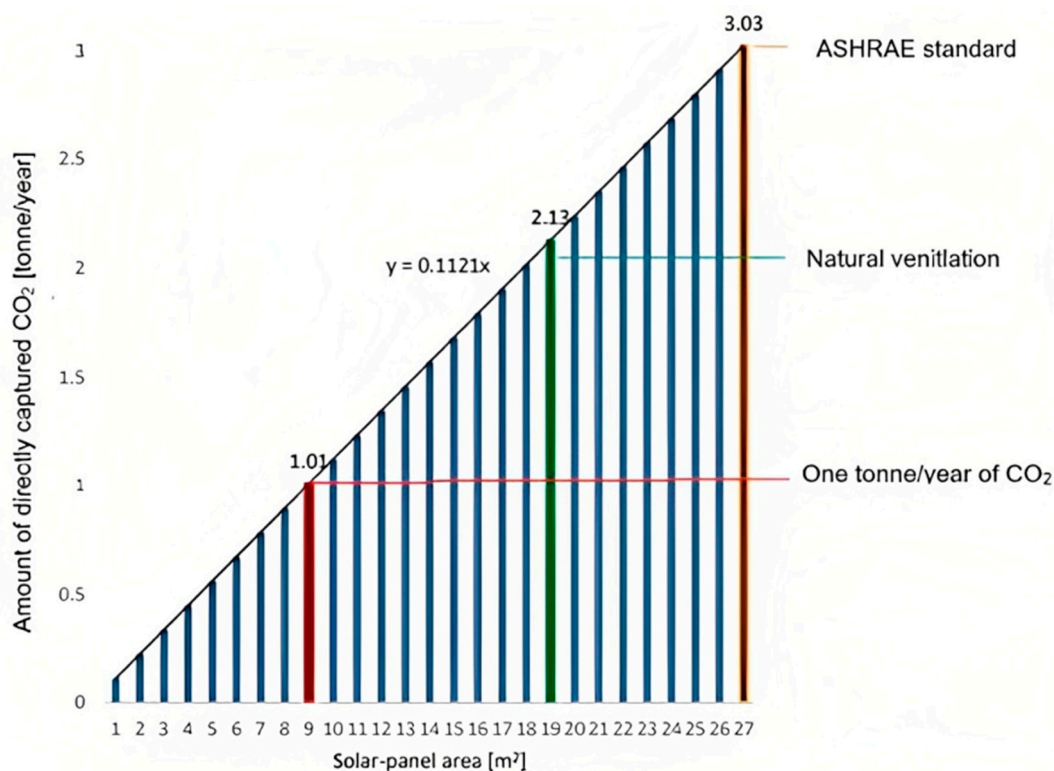


Figure 11. The total CO₂ amount captured annually through powering the DAC system by a photovoltaic system with a solar panel area of 1–27 m².

4. Conclusions

As motivation for individuals to adopt DAC systems, we propose a photovoltaic-powered DAC system that directly reduces CO₂ concentrations in a residential building. The airflow in the building was simulated using CFD and the energy performance analysis was undertaken using DesignBuilder. The CFD model was validated using microclimate-air quality dataloggers. The performance of the system has been quantified in various cases. To decarbonize the airflow supplied to the building by natural ventilation or ventilation according to the recommended ASHRAE standard, the photovoltaic system should generate 5.22 MW/year (solar panel area: 19 m²) or 7.4 MW/year (solar panel area: 27 m²), respectively. This corresponds, respectively, to 2.13 or 3.03 tons/year of CO₂, captured. Finally, the system's sensitivity has been determined: the captured amount of CO₂ with respect to the solar-panel area $\partial m_{CO_2} / \partial A_{PV} = 0.112$ tons/year·m². The power sensitivity of the photovoltaic system with respect to the solar-panel area $\partial P_{act} / \partial A_{PV} = 0.275$ MW/year·m².

This study analyzed a preliminary design of a photovoltaic-powered DAC system; in future work, it is crucial to consider other aspects, including the synchronization of the power supply to the power demand. This would involve integrating electricity storage techniques into the DAC system. In addition, while this study has determined the system's performance for a wide interval of decarbonizing capacity (solar panel area of 1–27 m², which corresponds to 0.275–3.03 tons/year of captured CO₂, respectively), the extent to which CO₂ is captured in a living space should be taken into consideration as another design-sizing criterion according to health guideline. It is noted that the results in this paper should be used in the context of a preliminary design process. In future work, the advanced design process shall consider more aspects. Carbon engineering typically uses a natural gas generator to produce a high-temperature (~800 °C) stream to dissociate CaCO₃ into CaO and CO₂ in the calciner. Thus, it should be ensured that the photovoltaic system can produce the temperature needed for CaCO₃ dissociation. Alternatively, a similar DAC process could be considered; for example, using the guanidine provided by Kasturi et al. [41], where the regeneration temperature is much lower (~130 °C).

Author Contributions: Conceptualization, A.H.A.A., O.F.A., L.M.L.P., L.E.-S., B.O., K.K., H.A. and A.I.A.; methodology, A.H.A.A., O.F.A., L.M.L.P., L.E.-S., B.O., K.K., H.A. and A.I.A.; software, A.H.A.A., O.F.A., L.M.L.P., L.E.-S., B.O., K.K., H.A. and A.I.A.; validation, A.H.A.A., O.F.A., L.M.L.P., L.E.-S., B.O., K.K., H.A. and A.I.A.; formal analysis, A.H.A.A., O.F.A., L.M.L.P., L.E.-S., B.O., K.K., H.A. and A.I.A.; investigation, A.H.A.A., O.F.A., L.M.L.P., L.E.-S., B.O., K.K., H.A. and A.I.A.; resources, A.H.A.A., O.F.A., L.M.L.P., L.E.-S., B.O., K.K., H.A. and A.I.A.; data curation, A.H.A.A., O.F.A., L.M.L.P., L.E.-S., B.O., K.K., H.A. and A.I.A.; writing—original draft preparation, A.H.A.A., O.F.A., L.M.L.P., L.E.-S., B.O., K.K., H.A. and A.I.A.; writing—review and editing, A.H.A.A., O.F.A., L.M.L.P., L.E.-S., B.O., K.K., H.A. and A.I.A.; visualization, A.H.A.A., O.F.A., L.M.L.P., L.E.-S., B.O., K.K., H.A. and A.I.A.; supervision, A.H.A.A., O.F.A., L.M.L.P., L.E.-S., B.O., K.K., H.A. and A.I.A.; project administration, A.H.A.A., O.F.A., L.M.L.P., L.E.-S., B.O., K.K., H.A. and A.I.A.; funding acquisition, A.H.A.A., O.F.A., L.M.L.P., L.E.-S., B.O., K.K., H.A. and A.I.A. All authors have read and agreed to the published version of the manuscript.

Funding: This research was funded by [the Qatar National Research Fund (a member of the Qatar Foundation)] grant number [No. NPRP13S-0203-200243] And The APC was funded by [e Qatar National Research Fund (a member of the Qatar Foundation)].

Acknowledgments: This publication was made possible by NPRP 13 Grant No. NPRP13S-0203-200243 from the Qatar National Research Fund (a member of the Qatar Foundation). The findings herein reflect the work and are solely the responsibility of the authors. Open Access funding is provided by the Qatar National Library.

Conflicts of Interest: The authors declare no conflict of interest.

Nomenclature

A_{PV}	The total area of the PV [m^2]
A_{act} / A_{PV}	Fraction of surface with active solar cells [%]
D	PV Depth [m]
	Direct Air Capture
m_{CO_2}	The annually captured CO_2 [tonne/year]
P_{Dac}	The required DAC power to capture 1 tonne of CO_2 [MW]
P_{act}	The required DAC power to capture CO_2 content from the actual natural ventilation airflow [MW]
P_{Dac} / V_{Dac}	The DAC power to air flow ratio to capture 1 tonne of CO_2 [MW/tonne]
\bar{P}_v	The total annual power generated by a $1\text{-}m^2$ solar-panel photovoltaic system [MW]
T	Temperature [K]
V_{act}	The actual natural ventilation rate supplied to the building [tonne/year]
V_{ASHRAE}	The required ventilation rate of the adopted generic building based on ASHRAE standards [tonne/year]
V_{Dac}	The corresponding air flow rate to capture 1 tonne of CO_2 [tonne/year]
V_x	Shear component of the wind velocity [m/s]
V_z	Normal component of the wind velocity [m/s]
$\partial P_{act} / \partial A_{PV}$	The power sensitivity of the photovoltaic system towards the solar-panel area [MW/ m^2]
$\partial m_{CO_2} / \partial A_{PV}$	The sensitivity of captured amount of CO_2 towards the solar-panel area [tonne/ m^2]
η_{pv}	PV efficiency [%]
η_I	Inventor efficiency [%]

Abbreviation

ASHRAE	The American Society of Heating, Refrigerating and Air-Conditioning Engineers
BECCS	Bio-energy carbon capture and storage
CCS	Carbon Capture and Storage
CFD	Computational Fluid Dynamic
COP	Coefficient of Performance
DAC	Direct Air Capture
IAM	Integrated assessment models
IPCC	Intergovernmental Panel on Climate Change
NE	Negative emission
NEES	Non-emitting energy sources

RE	Renewable energy
TSA	Temperature swing adsorption method
VCR	Vapor compression refrigeration
VRE	Variable renewable energy
UNFCCC	United Nations Framework Convention on Climate Change

References

- Kriegler, E.; Bauer, N.; Popp, A.; Humpenöder, F.; Leimbach, M.; Strefler, J.; Baumstark, L.; Bodirsky, B.L.; Hilaire, J.; Klein, D.; et al. Fossil-fueled development (SSP5): An energy and resource intensive scenario for the 21st century. *Glob. Environ. Chang.* **2017**, *42*, 297–315. [[CrossRef](#)]
- Rogelj, J.; Popp, A.; Calvin, K.V.; Luderer, G.; Emmerling, J.; Gernaat, D.; Fujimori, S.; Strefler, J.; Hasegawa, T.; Marangoni, G.; et al. Scenarios towards limiting global mean temperature increase below 1.5 °C. *Nat. Clim. Chang.* **2018**, *8*, 325–332. [[CrossRef](#)]
- Williamson, P. Emissions reduction: Scrutinize CO₂ removal methods. *Nature* **2016**, *530*, 153–155. [[CrossRef](#)]
- Intergovernmental Panel on Climate Change. 2018. Available online: www.ipcc.ch (accessed on 15 December 2018).
- Harper, A.B.; Powell, T.; Cox, P.M.; House, J.; Huntingford, C.; Lenton, T.M.; Sitch, S.; Burke, E.; Chadburn, S.E.; Collins, W.J.; et al. Land-use emissions play a critical role in land-based mitigation for Paris climate targets. *Nat. Commun.* **2018**, *9*, 2938. [[CrossRef](#)] [[PubMed](#)]
- Fajardy, M.; Mac Dowell, N. The energy return on investment of BECCS: Is BECCS a threat to energy security? *Energy Environ. Sci.* **2018**, *11*, 1581–1594. [[CrossRef](#)]
- Fridahl, M.; Mariliis, L. Bioenergy with carbon capture and storage (BECCS): Global potential, investment preferences, and deployment barriers. *Energy Res. Soc. Sci.* **2018**, *42*, 155–165. [[CrossRef](#)]
- King, L.C.; van den Bergh, J.C.J.M. Implications of net energy-return-on-investment for a low-carbon energy transition. *Nat. Energy* **2018**, *3*, 334–340. [[CrossRef](#)]
- Jacobson, M.Z.; Delucchi, M.A.; Bauer, Z.A.F.; Goodman, S.C.; Chapman, W.E.; Cameron, M.A.; Bozonnat, C.; Chobadi, L.; Clonts, H.A.; Enevoldsen, P.; et al. 100% Clean and Renewable Wind, Water, and Sunlight All-Sector Energy Roadmaps for 139 Countries of the World. *Joule* **2017**, *1*, 108–121. [[CrossRef](#)]
- Jacobson, M.Z.; Cameron, M.A.; Hennessy, E.M.; Petkov, I.; Meyer, C.B.; Gambhir, T.K.; Maki, A.T.; Pflieger, K.; Clonts, H.; McEvoy, A.L.; et al. 100% clean and renewable Wind, Water, and Sunlight (WWS) all-sector energy roadmaps for 53 towns and cities in North America. *Sustain. Cities Soc.* **2018**, *42*, 22–37. [[CrossRef](#)]
- Brown, T.W.; Bischof-Niemz, T.; Blok, K.; Breyer, C.; Lund, H.; Mathiesen, B.V. Response to “Burden of proof: A comprehensive review of the feasibility of 100% renewable-electricity systems”. *Renew. Sustain. Energy Rev.* **2018**, *92*, 834–847. [[CrossRef](#)]
- Breyer, C.; Bogdanov, D.; Aghahosseini, A.; Gulagi, A.; Child, M.; Oyewo, A.S.; Farfan, J.; Sadovskaia, K.; Vainikka, P. Solar photovoltaics demand for the global energy transition in the power sector. *Prog. Photovolt. Res. Appl.* **2018**, *26*, 505–523. [[CrossRef](#)]
- Child, M.; Koskinen, O.; Linnanen, L.; Breyer, C. Sustainability guardrails for energy scenarios of the global energy transition. *Renew. Sustain. Energy Rev.* **2018**, *91*, 321–334. [[CrossRef](#)]
- Fogarty, J.; Michael, M. Health and safety risks of carbon capture and storage. *JAMA* **2010**, *303*, 67–68. [[CrossRef](#)] [[PubMed](#)]
- Creutzig, F.; Peter, A.; Jan, C.G.; Gunnar, L.; Gregory, N.; Robert, C.P. The underestimated potential of solar energy to mitigate climate change. *Nat. Energy* **2017**, *2*, 17140. [[CrossRef](#)]
- Leung, D.Y.C.; Caramanna, G.; Maroto-Valer, M.M. An overview of current status of carbon dioxide capture and storage technologies. *Renew. Sustain. Energy Rev.* **2014**, *39*, 426–443. [[CrossRef](#)]
- Monastersky, R. Seabed scars raise questions over carbon-storage plan. *Nature* **2013**, *504*, 339–340. [[CrossRef](#)]
- Jiang, L.; Liu, W.; Wang, R.Q.; Gonzalez-Diaz, A.; Rojas-Michaga, M.F.; Michailos, S.; Pourkashanian, M.; Zhang, X.J.; Font-Palma, C. Sorption direct air capture with CO₂ utilization. *Prog. Energy Combust. Sci.* **2023**, *95*, 101069. [[CrossRef](#)]
- Ying; Yong, J.; Liu, W.; Zhang, X.; Jiang, L. Thermodynamic analysis on direct air capture for building air condition system: Balance between adsorbent and refrigerant. *Energy Built Environ.* **2023**, *4*, 399–407.
- DS Limited. DesignBuilder 2.1. *User’s Manual2009*. Available online: http://www.designbuildersoftware.com/docs/designbuilder/DesignBuilder_2.1_Users-Manual_Ltr.pdf (accessed on 2 October 2021).
- BIBlanco, J.M.; Buruaga, A.; Rojí, E.; Cuadrado, J.; Pelaz, B. Energy assessment and optimization of perforated metal sheet double skin façades through Design Builder; A case study in Spain. *Energy Build.* **2016**, *111*, 326–336. [[CrossRef](#)]
- DS Limited. ASHRAE 140-2017/BESTEST Results for DesignBuilder v6.12021. Available online: <https://designbuilder.co.uk/download/documents> (accessed on 28 March 2022).
- Judkoff, R.; Neymark, J. *International Energy Agency Building Energy Simulation Test (BESTEST) and Diagnostic Method*; National Renewable Energy Lab.: Golden, CO, USA, 1995. [[CrossRef](#)]
- Alrebei, O.F.; Le Page, L.M.; McKay, G.; El-Naas, M.H.; Amhamed, A.I. Recalibration of carbon-free NH₃/H₂ fuel blend process: Qatar’s roadmap for blue ammonia. *Int. J. Hydrogen Energy* **2023**, *in press*. [[CrossRef](#)]
- Crawley, D.; Lawrie, L. Repository of Free Climate Data for Building Performance Simulation. 2018. Available online: https://climate.onebuilding.org/WMO_Region_2_Asia/QAT_Qatar/index.html (accessed on 10 March 2022).
- Fawwaz Alrebei, O.; Obeidat, L.M.; Ma’bdeh, S.N.; Kaouri, K.; Al-Radaideh, T.; Amhamed, A.I. Window-Windcatcher for Enhanced Thermal Comfort, Natural Ventilation and Reduced COVID-19 Transmission. *Buildings* **2022**, *12*, 791. [[CrossRef](#)]

27. Mabdeh, S.; Al Radaideh, T.; Hiyari, M. Enhancing Thermal Comfort of Residential Buildings Through a Dual Functional Passive System (SOLAR-WALL). *J. Green Build.* **2021**, *16*, 155–177. [[CrossRef](#)]
28. Weatherspark. Available online: <https://weatherspark.com/> (accessed on 30 December 2021).
29. Alrebi, O.F.; Obeidat, B.; Abdallah, I.A.; Darwish, E.F.; Amhamed, A. Airflow dynamics in an emergency department: A CFD simulation study to analyse COVID-19 dispersion. *Alex. Eng. J.* **2022**, *61*, 3435–3445. [[CrossRef](#)]
30. Obeidat, B.; Alrebei, O.F.; Abdallah, I.A.; Darwish, E.F.; Amhamed, A. CFD Analyses: The Effect of Pressure Suction and Airflow Velocity on Coronavirus Dispersal. *Appl. Sci.* **2021**, *11*, 7450. [[CrossRef](#)]
31. Available online: <https://www.deltaohm.com/product/hd32-3tc-thermal-microclimate-pmv-ppd-wbgt/> (accessed on 15 January 2023).
32. Available online: <https://www.deltaohm.com/product/ap3203f-omnidirectional-hotwire-probe-2/> (accessed on 15 January 2023).
33. Bartak, M.; Beausoleil-Morrison, I.; Clarke, J.; Denev, J.; Drkal, F.; Lain, M.; Macdonald, I.; Melikov, A.; Popiolek, Z.; Stankov, P. Integrating CFD and building simulation. *Build. Environ.* **2002**, *37*, 865–871. [[CrossRef](#)]
34. Nouh Ma'bdeh, S.; Fawwaz Alrebei, O.; Obeidat, L.M.; Al-Radaideh, T.; Kaouri, K.; Amhamed, A.I. Quantifying energy reduction and thermal comfort for a residential building ventilated with a window-windcatcher: A case study. *Buildings* **2023**, *13*, 86. [[CrossRef](#)]
35. Li, Y.; Nielsen, P.V. CFD and ventilation research. *Indoor Air* **2011**, *21*, 442–453. [[CrossRef](#)] [[PubMed](#)]
36. Alrebei, O.F.; Obeidat, B.; Al-Radaideh, T.; Le Page, L.M.; Hewlett, S.; Al Assaf, A.H.; Amhamed, A.I. Quantifying CO₂ Emissions and Energy Production from Power Plants to Run HVAC Systems in ASHRAE-Based Buildings. *Energies* **2022**, *15*, 8813. [[CrossRef](#)]
37. Liu, J.; Niu, J. CFD simulation of the wind environment around an isolated high-rise building: An evaluation of SRANS, LES and DES models. *Build. Environ.* **2016**, *96*, 91–106. [[CrossRef](#)]
38. Alrebei, O.F.; Le Page, L.M.; Hewlett, S.; Bicer, Y.; Amhamed, A. Numerical investigation of a first-stage stator turbine blade subjected to NH₃–H₂/air combustion flue gases. *Int. J. Hydrogen Energy* **2022**, *47*, 33479–33497. [[CrossRef](#)]
39. Zhai, Z.J.; Chen, Q.Y. Performance of coupled building energy and CFD simulations. *Energy Build.* **2005**, *37*, 333–344. [[CrossRef](#)]
40. Obeidat, L.M.; Alrebei, O.F.; Nouh Ma'bdeh, S.; Al-Radaideh, T.; Amhamed, A.I. Parametric Enhancement of a Window-Windcatcher for Enhanced Thermal Comfort and Natural Ventilation. *Atmosphere* **2023**, *14*, 844. [[CrossRef](#)]
41. Kasturi, A.; Jang, G.G.; Stamberg, D.; Custelcean, R.; Yiacoumi, S.; Tsouris, C. Determination of the regeneration energy of direct air capture solvents/sorbents using calorimetric methods. *Sep. Purif. Technol.* **2023**, *310*, 123154. [[CrossRef](#)]

Disclaimer/Publisher's Note: The statements, opinions and data contained in all publications are solely those of the individual author(s) and contributor(s) and not of MDPI and/or the editor(s). MDPI and/or the editor(s) disclaim responsibility for any injury to people or property resulting from any ideas, methods, instructions or products referred to in the content.